SSC DRIFT TUBE LINAC PHYSICS DESIGN*

G. Neuschaefer, S. Nath, J. Billen, and T. Bhatia
Los Alamos National Laboratory, Los Alamos, NM 87545
J. Watson
Superconducting SuperCollider Laboratory, Dallas, TX

Abstract

This paper describes the present status of the beam-dynamics design for the SSC drift-tube linac (DTL). The DTL is designed to accelerate a H^- beam from 2.5 MeV to 70 MeV. The design beam current is 25 mA at 428 MHz. The DTL consists of four tanks stabilized by post couplers. Transverse focusing is provided by permanent magnet quadrupoles (PMQs). Intertank longitudinal matching is provided by displaced end-cell rf gaps. The rf field is ramped in Tank 1 but is held constant through the remainder of the DTL. A brief description of the beam dynamics and structures issues is presented here. Details on these aspects will be available in a forthcoming report.

Physics Issues

A radio frequency quadrupole (RFQ) is expected to provide the DTL with a 25 mA, H^- beam of rms normalized emittance $\varepsilon = 0.02\ \pi$ cm·mrad in both the transverse and longitudinal phase spaces. The zero current longitudinal and transverse focusing strengths per unit physical length at the entrance of the 428-MHz DTL are chosen to be similar to those at the 428-MHz RFQ exit. This makes a nearly current independent "RFQ to DTL" matching section feasible. Accordingly the transverse and longitudinal phase advance per $\beta\lambda$ at zero current are kept approximately at 20° and 13.5° respectively throughout Tank 1. Although ramping[1] the rf field (E_0T) throughout the DTL will shorten the linac, power and peak surface field requirements limit this approach. In the present design, we choose to ramp E_0T and the synchronous phase (ϕ_s) only in Tank 1. This rf ramp prescription was first used in the Los Alamos proof-of-principal RFQ gentle buncher section.

The DTL starts with $\phi_s = -35°$ which is the same as at the RFQ exit. It is then ramped to –30° for more efficient acceleration using

$$\psi^o = \psi^o_{init}\,(\beta_{init}/\beta)\,, \qquad (1)$$

where ψ^o is the zero current longitudinal separatrix width in units of rf degrees, and β is the particle velocity divided by the speed of light; ϕ_s and ψ^o are related by

$$\tan\phi_s = (\sin\psi^o - \psi^o)/(1 - \cos\psi^o)\,. \qquad (2)$$

*Work supported and funded by the US Department of Energy, Office of Superconducting SuperCollider.

This ψ^o ramp holds ψ^ℓ, the width of ψ in units of length, constant. After ϕ_s attains the value of –30° in Tank 1, it is held constant, allowing ψ^ℓ to increase. E_0T is ramped from 1.5 MV/m (same as at the RFQ exit) to 4.0 MV/m. The final E_0T, 4.0 MV/m, is set by the limit on the peak surface electric field. A linear ramp approximates the E_0T ramp defined by the following equation:

$$E_0T\sin\phi_s/(\beta\gamma^3) = \text{Constant}\,, \qquad (3)$$

where

E_0 is the average accelerating field over a cell,
T is the transit time factor, and
$\gamma = (1-\beta^2)^{-0.5}$.

The above prescription keeps the longitudinal beam size (in units of length) in Tank 1 approximately constant. Keeping the beam size approximately constant throughout the DTL prevents emittance growth from energy exchange between the longitudinal and transverse phase spaces. In Tanks 2, 3, and 4, E_0T is held constant at 4.0 MV/m and $\phi_s = -30°$. This results in a slow longitudinal expansion of the beam size in real space.

Transverse focusing is provided by PMQs. Two focusing lattices, FODO and FOFODODO were examined. We simulated, in addition to the design beam of 25 mA, a high- and low-emittance 75-mA beam to observe the DTL's sensitivity to current and emittance. Table 1 shows very little emittance growth in all cases. Both transverse focusing schemes yield similar beam sizes when random quadrupole misalignments are included. Tank 1 PARTRACE[2] calculations[3] were done for both the schemes with ±0.005 inch random (uniform distribution) quadrupole transverse misalignments.

Table 1
Normalized rms emittance in π cm·mrad
(simulated as one tank from 2.5 to 70 MeV)

Focusing Scheme	Current mA	2.5 MeV Input Beam		70 MeV Output Beam		Zero Current Transverse Phase Advance per Cell (degree)
		ε_t	ε_ℓ	ε_t	ε_ℓ	
fodo	25	0.020	0.020	0.020	0.022	23
fodo	75	0.060	0.060	0.060	0.063	23
fodo	75	0.010	0.010	0.010	0.024	23
fofododo	25	0.020	0.020	0.020	0.023	20
fofododo	75	0.060	0.060	0.065	0.064	20
fofododo	75	0.010	0.010	0.011	0.020	20

For a FOFODODO lattice there is a 99% probability that the beam outer edge will not exceed 0.63 cm (centroid displacement = 0.33 cm) when the beam enters in the geometric tank center. A FODO lattice has a 99% probability maximum beam edge radius of 0.64 cm. PMQ constraints limit the FODO bore radius to ~0.65 cm, however, the FOFODODO radius can be 1.1 cm. This led to the choice of a FOFODODO lattice. The beam (0.02 π cm·mrad, 25 mA) width in these calculations was taken to be 3 times the rms size. Tanks 2, 3, and 4 have fewer cells and therefore are less sensitive to magnet misalignments.

Drift Tubes

The design of individual cells in a tank was carried out using SUPERFISH[4]. A typical drift-tube shape is shown in Figure 1. Parameters are given in Table 2. The design of these drift-tubes was constrained by several interrelated factors: (a) the desirability of a large bore size, (b) a peak surface field (E_p) not to exceed 1.4 Kilpatrick field (E_k), (c) tank power not to exceed 3 MW, and (d) PMQs of required strength. The 'rf gap length' to 'cell length' was varied from cell to cell to attain the resonating frequency of 428 MHz. The DTL parameters for Tanks 1 through 4 are shown in Table 3.

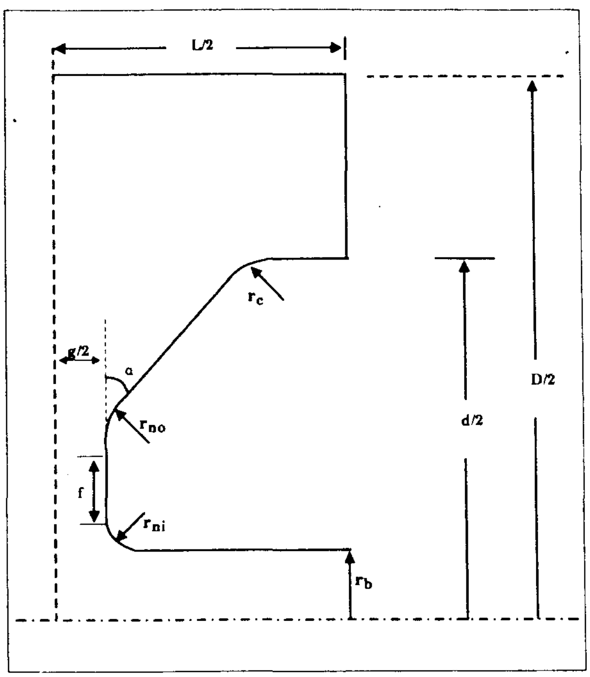

Fig. 1. Schematic cross-section of a drift tube. L: cell length, D: tank diam., d: drift-tube diam., r_b bore radius, g: gap length, f: flat face length, r_{ni}: inner nose radius, r_{no}: outer nose radius, and r_c: corner radius, and α: face angle.

Permanent Magnet Quadrupoles (PMQs)

Typical shapes for PMQs, to be made out of Sm_2Co_{17}, are shown in Fig. 2. The pertinent parameters are given in Table 4. Data for the variation[5] of the magnetic field gradient along the axis of a real (soft edge) quadrupole are used as input to TRACE3D[6] to calculate the beam phase advance, including overlapping magnetic fields and rf defocusing. The quadrupole gradients must be varied to maintain $\sigma_{ot} \simeq 80°$ as the energy goes up from 2.5 MeV to 70 MeV. The variation must be smooth to prevent beam mismatch. The DTL transverse and longitudinal tune depressions σ/σ_0 are 0.75 and 0.61, where σ is the phase advance per focussing period at 25 mA. In between the tanks there is a 3βλ drift space. In order to maintain a smooth variation in longitudinal beam size through this 3βλ drift space the tank exit rf-gaps and

Table 2
Drift Tube Parameters

	Tank 1	Tank 2 & 3	Tank 4
L (cm)	5.1-12.2	12.2–22.4	22.4–25.6
D (cm)	44.0	42.0	42.0
g (cm)	1.2-4.6	2.6-8.2	8.1-10.2
d (cm)	14.0	8.0	8.4
r_c (cm)	1.0	1.0	1.0
r_{no} (cm)	1.0	0.75	0.75
r_{ni} (cm)	0.50	0.50	0.50
r_b (cm)	1.10	0.9	0.9
α (deg)	11.0	15.0	18.0
f (cm)	0.2	0.2	0.1

Table 3
DTL Design Parameters

Tank No.	Transit Time	Peak Field Ep/Ek	Power* MW	Number Cells	Bore Radius cm	EoT MV/m	Tank – Tube dia in λ/4	Tank dia cm
1	.55-.68	0.71-1.12	2.34	62	1.1	1.5-4.0	0.86	44.0
2	.84-.80	1.38-1.23	2.78	40	0.9	4.0	0.97	42.0
3	.80-.75	1.23-1.33	2.69	26	0.9	4.0	0.97	42.0
4	.75-.71	1.25-1.36	2.94	22	0.9	4.0	0.96	42.0

*Includes 25 mA beam + 1.3 × SUPERFISH + tank endwalls

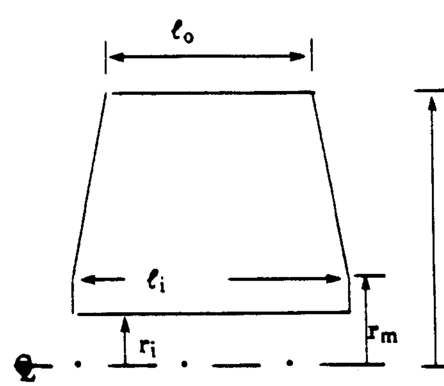

Fig. 2. Schematic cross-section of a PMQ. r_i = inner radius, r_o = outer radius, r_m = mid radius, ℓ_i = inner length, and ℓ_o = outer length.

Table 4
FOFODODO MAGNETS

	Tank 1	Tank 2 thru 4
r_i (cm)	1.30	1.10
r_o (cm)	6.00	2.50
r_m (cm)	2.00	1.70
ℓ_i (cm)	2.80	3.10
ℓ_o (cm)	1.30	2.40
$<B_r>$ (KG)*	10.00	10.00
$\int G.dl$ (KG)	28.7	28.6
Pole Tip Field (KG)	10.97	9.72

* $
 = (B_r + H_c)/2$

entrance rf-gaps are shifted w.r.t the PMQs to provide additional focusing.

Two mechanically adjustable gradient PMQ's between the tanks provide transverse focusing and also provide 2 knobs to match the beam's transverse Twiss parameters to the next tank. These quadrupoles will also be transversely movable to provide beam steering. Each tank end may also need to be independently movable to provide position adjustment into the next tank's displaced (in the presence of drift tube misalignments) acceptance.

Simulation Results

With the DTL geometry and field configuration discussed above, the linac simulation code PARMILA[7] was run with 1000 macroparticles to examine the beam dynamics at 25 mA. The input phase-space distribution was that of a uniformly filled six-dimensional hyperellipsoid. Figure 3 shows the beam's horizontal and longitudinal dimensions as it traverses the DTL, along with its energy spread. As can be seen, the beam transverse and longitudinal dimension is approximately constant at all points in the accelerator and exhibits the size oscillation typical of an alternating gradient focusing system. The bunch length in rf degrees decreases from $\pm 16°$ to about $\pm 4°$ at the end of linac and energy spread increases to about $\pm$ 150 keV. Emittance (4 tank) results are shown in Table 5. There is very little growth in both ε_t and ε_ℓ with $\sigma_{ot} = 80°$.

Simulation (one tank to 70 MeV) results with $\sigma_{ot} = 60°$, 70°,and 85° (4$\beta\lambda$ FOFODODO period) are approximately the same as with $\sigma_{ot} = 80°$. But at $\sigma_{ot} = 90°$ the envelope instability[8] appears resulting in a transverse beam halo and increased emittance growth.

Post Couplers

The DTL fields will be stabilized by resonant post couplers. Excellent stability can be provided by placing post couplers adjacent to every other full drift tube. The post couplers protrude into the tank at right angles to the drift-tube stems alternating from side to side. Each tank has an even number of cells to facilitate this placement scheme. In traditional post-coupler-stabilized DTLs, the tank diameter D and the drift-tube diameter d are constrained to a narrow range by the relation[9]

$$0.9\,(\lambda/4) < (D-d)/2 < 1.03\,(\lambda/4)\,, \qquad (4)$$

where λ is the free-space wavelength corresponding to the cavity operating mode frequency.

Tanks 2, 3, and 4 of the DTL were designed with (D-d)/2 within the range given in Eq. 4. Tank 1 has (D-d)/2 = 0.86 (λ/4), which is just below the range in Eq. 4. Because the post couplers in Tank 1 will be shorter than those in the other tanks they are likely to be too high in frequency if the same tip design for the post is used. A slightly larger tab can be used on Tank 1 post couplers to lower the tuning range.

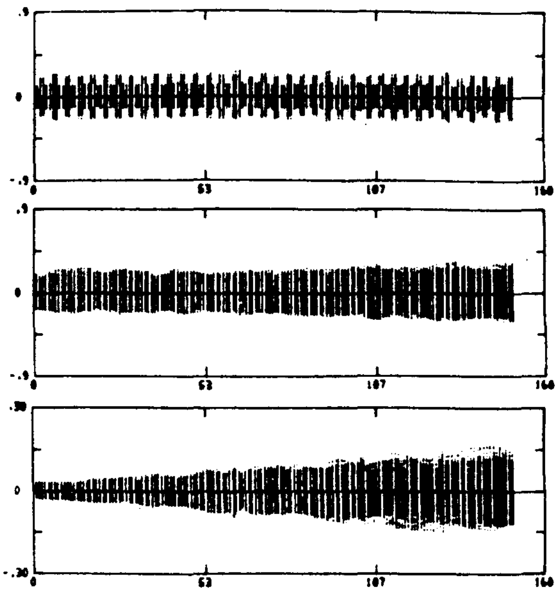

Fig. 3. Simulated DTL beam properties vs cell number.
Top: Horizontal Dimension (cm)
Middle: Bunch Length (cm)
Bottom: Energy Spread (MeV)

Table 5
Normalized rms Emittance in π cm·mrad
(Four Tank Simulation)

Focusing Scheme	Current (mA)	2.5MeV Input Beam		70MeV Output Beam		Zero current transverse phase advance per cell (degree)
		ε_t	ε_ℓ	ε_t	ε_ℓ	
fofododo	25	0.0204	0.0210	0.0198	0.0214	20

Frequency Shifts and Frequency Errors

The drift-tube stems, post couplers, dynamic tuners, and static tuning bars all tend to raise the cavity frequency. The coupling iris and any holes for pumping have the opposite effect. After the basic geometry has been determined, a small adjustment of the tank radius corrects for net frequency shift to ensure operation at 428 MHz.

We distinguish between these frequency shifts and frequency errors, which result from differences within machining tolerances between the as-built cavity geometry and the design geometry. Two static tuning bars will be provided in each tank to correct for the largest frequency errors expected. More than half of the potential frequency error results from the mechanical tolerance of $\pm.002$ inches on the drift-tube length. Other major contributions come from the $\pm.010$-inch tolerance on the tank diameter ($\sim 22\%$) and the ± 0.003 inch tolerance on the drift-tube diameter ($\sim 17\%$). Both frequency shifts and frequency errors are derived using the Slater perturbation theorem[10].

Longitudinal Field Distribution

The beam-dynamics design provides for a ramped field distribution in Tank 1 and for a constant or "flat" field in Tanks 2, 3, and 4. For graded-β DTLs, the stem frequency effect on individual cells is larger on the low-energy (LE) end of the tank than on the high-energy (HE) end. This continuous detuning of cells along the cavity length produces a naturally ramped longitudinal field distribution, increasing in field strength toward the HE end. A calculation of the stem-produced cell-frequency differences combined with a measurement of the tank's tilt sensitivity gives an estimate of the resulting end-to-end field ramp.

To achieve the design field in each tank, the end cells will be detuned by slightly varying the drift-tube face angle of the end-wall half drift tube from the design face angle used throughout the tank. This procedure helps to simplify low-power tuning of the structure by reducing the level of excitation of the post couplers necessary to stabilize the design field distribution. With a high level of post-coupler excitation, the post couplers' dual functions of stabilization and field trimming tend to interfere with one another. Thus, in Tanks 2, 3, and 4, the stem-produced ramp will be removed by the end-cell detuning procedure, and in Tank 1, the end cells will be detuned to make up the difference between the design ramp and the stem-produced ramp.

Summary

The DTL physics design outlined above provides an excellent scheme for acceleration from 2.5 to 70 MeV with an output-beam of high quality. There is essentially zero growth (in the absence of fabrication errors) in emittance for the design beam, and the particles occupy less than one-third of the bore size for a uniform input beam. The design power requirement for each tank is less than 75% of the available power of 4MW. The design and materials for the drift tubes and magnet structures are all within the scope of available technology. The 4 tank DTL is 23.48 m long. The following considerations, among others, demand careful attention.

Careful measurements on the PMQs must be made in order to insure $75° \leq \sigma_{0t} \leq 80°$ before drift tubes are welded around them. In designing the drift tubes with SUPERFISH, the mesh size used ranged from 0.025 cm to 0.045 cm. Regeneration of cell sizes with a finer mesh will be necessary before fabrication. Future studies are necessary to coordinate "engineering designs, fabrication specifications & control systems" with "beam-dynamics performance, tune up and operation requirements". Adequate beam diagnostics between the tanks are vital for transverse matching and rf control during commissioning and routine operation. Although not planned for at this time, it is possible to split a drift tube quadrupole and put a microstrip probe in the middle of a drift tube. When the drift tube minus quadrupole length is large enough for microstrip probes, every 4th cell, for example, could be equipped with a probe to track the beam centroid through a tank. This tracking can serve as an alternate method for measuring the acceptance rather than steering the beam to observe a drop in transmission. Emittance growth and bore used can be significantly minimized by placing the beam in the center of a tank's displaced acceptance.

References

1. T. P. Wangler, "Physics Design of Linear Accelerators for Intense Ion Beams", Proceedings of the Linear Acclerator Conference, Williamsburg, VA, Oct 3-7,1988, Los Alamos National Laboratory document LA-UR-88-3231.
2. K. R. Crandall, "Error studies using Partrace, A new program that combines PARMILA and TRACE 3-D", 1988 Linear Accelerator Conference, Williamsburg, VA., October 3-7, 1988
3. S. Nath, G. Neuschaefer, "SSC DTL Tank 1 Design", Los Alamos National Laboratory memorandum AT-1:90-231.
4. K. Halbach and R. F. Holsinger, "SUPERFISH - A Computer Program for Evaluation of RF Cavities with Cylindrical Symmetry," Los Alamos National Laboratory memorandum AT-6-TM:89-37.
5. G. P. Boicourt, J. L. Merson, "Calculations on Permanent Magnet Quadrupoles with Nonrectangular Cross Sections," Los Alamos National Laboratory document LA-UR-88-3149.
6. K. R. Crandall, "TRACE 3-D Documentation," Los Alamos National Laboratory document LA-11054-MS.
7. G. P.Boicourt, "PARMILA - An Introduction Workshop on Linear Accelerators and Beam Optics Codes," AIP conference Proccedings, San Diego, CA, January 19-21, 1988, Los Alamos National Laboratory document LA-UR-88-1544.
8. L. Smith, L. J. Laslett, I. Hofmann, and I. Haber, "Stability of KV Distributions in Long Periodic Systems," Particle Accelerators 13 (1983) 145.
9. J.H. Billen, "Survey of Drift-Tube Linacs with Post Couplers," Los Alamos National Laboratory memorandum AT-1:84-74.
10. E. L. Ginzton, Microwave Measurements, McGraw-Hill, 1957, Chapter 10.